Hydrol. Earth Syst. Sci. Discuss., 5, 3383–3418, 2008
www.hydrol-earth-syst-sci-discuss.net/5/3383/2008/

Hydrology and Earth System Sciences Discussions

Papers published in *Hydrology and Earth System Sciences Discussions* are under open-access review for the journal *Hydrology and Earth System Sciences*

On the derivation of soil surface roughness from multi parametric PolSAR data and its potential for hydrological modelling

P. Marzahn and R. Ludwig

Department of Geography, Ludwig-Maximilian University Munich, Germany

Received: 26 September 2008 – Accepted: 29 September 2008
– Published: 28 November 2008

Correspondence to: P. Marzahn (p.marzahn@iggf.geo.uni-muenchen.de)

Published by Copernicus Publications on behalf of the European Geosciences Union.

Abstract

The potential of multi parametric polarimetric SAR (PolSAR) data for soil surface roughness estimation is investigated and its potential for hydrological modeling is evaluated. The study utilizes microwave backscatter collected from the DEMMIN test-site in the north-east of Germany during the AgriSAR 2006 campaign using fully polarimetric L-Band E-SAR data. In addition to various measurements of soil physical properties, soil surface roughness was measured extensively using photogrammetric image matching techniques for ground truthing. The resulting micro-DEMs are analyzed to correlate soil surface roughness indices to three well established polarimetric roughness estimators. Good results are obtained for $Re_{[\rho \mathrm{RRLL}]}$ vs. RMS Height, which is thus used to produce multi-temporal roughness maps of the test site. The spatial quality of maps is limited due to the fact that the presence and growth of particular plants is affecting the derivation process significantly. However, roughness derivation for bare soil surfaces is sufficiently accurate to allow for an first order assessment of soil-hydrological parameters (soil porosity, void ratio, micro depression storage capacity), which are crucial for the initialization and operation of hydrological surface models. While uncertainties remain, the dependency of soil bulk parameters from surface roughness can be shown and thus highlights the potential of the retrieval approach for hydrological model applications.

1 Introduction

At the boundary between the atmosphere and the pedosphere, soil surface roughness plays an important role in numerous physical processes related to water, energy and nutrient flux and exchange. This has been widely recognized in novel land surface modelling efforts. On cultivated soils, many studies have demonstrated that different roughness states influence runoff generation and formation due to soil sealing and crusting effects (Fohrer et al., 1999). Furthermore, processes like infiltration, evap-

HESSD

5, 3383–3418, 2008

oration, soil erosion by wind and water, lateral and vertical matter fluxes, as well as the growth and vitality of particular agricultural plants are all influenced by soil surface roughness states and its resulting changes in soil bulk density, respectively the soil void ratio in the upper few centimetres of the soil column (Farres, 1980; Helming, 1992; Le Bissionais et al., 1998; Fohrer et al., 1999; Cerdan et al., 2001; Darboux et al., 2002; Zeiger, 2007).

Changes in soil surface roughness conditions take place due to agricultural practice or are related to precipitation and wind effects. While meteorological impacts cause a smoothing in roughness states and an increase in bulk density, agricultural practice produces different roughness states depending on the tillage tool used. Allmaras et al. (1966) defined two different roughness terms with regard to their geometrical appearance: orientated and random roughness. While orientated roughness is dependent on the tillage tool or general slope effects, the random roughness is caused by the fortuitous occurrence of peaks and depressions resulting from soil clods and organization of aggregates which cannot be addressed to orientated roughness (Allmaras et al., 1966). Römkens and Wang (1986) defined the random roughness alongside other scale depending roughness types as the height deviations from a reference plain in the scale of 2–200 mm.

For soil surface roughness characterization on small plots up to 16 m^2, different roughness indices have been proposed and successfully utilized (Allmaras et al., 1966; Betuzzi, 1990; Taconet and Ciarletti, 2006; Zeiger, 2007). However, the direct measurement of soil surface roughness on the field scale is not yet appropriately dissolved. This is leading to strong simplification and considerable data uncertainty in the description of spatial soil surface roughness conditions in recent physically based runoff generation modelling efforts on the catchment scale. While expensive and labor intensive in-situ measurements are limited to small areas, remote sensing techniques are able to cover larger areas at relatively high frequency, which might offer the opportunity to measure dynamic soil surface characteristics on larger scales (Santanello et al., 2007; Loew and Mauser, 2008). In this study, the derivation of soil surface roughness infor-

mation on field scale is conducted and evaluated from multi temporal airborne PolSAR data. To investigate the application potential in hydrological modelling, the deployment of multi temporal soil surface roughness maps for the retrieval of micro scale depression storage capacity and soil physical parameters, such as bulk density and void ratio, are presented as first results of a feasibility study.

2 Methods and field data

The study was performed in the frame of the ESA-founded campaign AgriSAR 2006, which was carried out from mid-April to the end of July at the DEMMIN (Durable Environmental Multidisciplinary Monitoring Information Network) test site (Hajnsek et al., 2007). A major component of this study was to generate an image and ground data base on a weekly basis for the examination and validation of bio-/geo-physical parameter retrievals and to simulate ESA's future Sentinel 1 and Sentinel 2 missions. Radar flights on a weekly basis with the well known E-SAR system operated by the German Aerospace Centre (DLR-HR) onboard a DO-228 were accompanied by extensive in-situ measurements.

2.1 Test site

DEMMIN is a consolidated test site in Mecklenburg-Western Pomerania in north-east Germany, approximately 150 km north of Berlin (Fig. 1). The $3 \times 8\,km^2$ test-site is located in the young moraine area, characterized by smooth topography and intensive agricultural cultivation on high productive soils. The altitudinal range within the test-site is about 60 m with its maximum in the north and a minimum in the southern parts of the test site near the Peene river. Soil texture ranges from sandy loam to loamy sand. The main crop rotation is winter wheat, winter rape and winter barley. Additionally, maize and sugar beet is sown in spring for livestock feed. The mean field size is 225 ha. Due to very large fields and intensive cultivation, some evidence of wind and water erosion

can be observed within the fields.

18 sample points were chosen to represent the main crops in the test site during the campaign. Figure 2 shows the location of the sample points. Most of the sampling points are situated in plain areas except for sample points (ESU) 102-1 (SB) and 222-2 (M) which are located in local sinks or in small drainage channels.

2.2 Radar acquisitions and processing

A total of 11 E-SAR flights were carried out on a weekly basis, recording imagery in X-, C-, and L-Band . The raw radar data was preprocessed radiometrically and geometrically at DLR-HR. The L-Band radar data showed good quality with an absolute error of –2 dB and a phase accuracy of 2° (Scheiber et al., 2007).

Geocoded SLC L-Band Data was chosen to retrieve the roughness information. As shown by Thiel et al. (2001) it is feasible to use E-SAR geocoded SLC L-Band data to perform polarimetric image analysis. Prior to further image analysis, the radar imagery was speckle filtered by applying a 7×7 window enhanced LEE-Filter, which corresponds to approximately 34 looks. Finally, three well established roughness estimators were calculated from the radar data.

Cloude (1999), Cloude and Lewis (2000) as well as Hajnsek et al. (2003) first introduced the Anisotropy as a potential roughness estimator, which is only dependent from the geometrical properties of a given surface and independent from its dielectric properties. The Anisotropy (A), defined as a ratio between the second (λ_2) and third (λ_3) eigenvalues (Cloude and Pottier, 1996), can be inverted using two different linear approaches, dependent on the roughness conditions.

$$A = \frac{\lambda_2 - \lambda_3}{\lambda_2 + \lambda_3} \tag{1}$$

For smooth areas Cloude and Lewis (2000) suggest:

$$ks = 1.25 - 2A \tag{2}$$

while for rougher surfaces Cloude (1999) recommended:

$$ks = 1 - A \tag{3}$$

As shown by Mattia et al. (1997) during different field experiments over the Matera test site (Italy) and the Chickasha test site (USA), the complex circular coherence ($|\rho_{RRLL}|$) is sensitive to roughness effects and insensitive to dielectric properties, respectively soil moisture of the illuminated target. The complex circular right-right left-left coherence is defined as:

$$|\rho_{RRLL}| = \frac{\langle |S_{RR} S_{LL}^{*}| \rangle}{\sqrt{\langle |S_{RR}|^2 \rangle \langle |S_{LL}|^2 \rangle}} \tag{4}$$

with S_{RR}=right-right rotation, S_{LL}=left-left rotation of the electric field vector about the line of sight.

In further investigations Schuler et al. (2002) approved this sensitivity of $|\rho_{RRLL}|$ but established a stronger relationship between the soil surface roughness and the real part of the circular coherence ($Re_{[\rho RRLL]}$) for a wide range of natural soil surfaces and different frequencies. The real part of the circular coherence is defined as (Schuler et al., 2002):

$$Re_{[\rho RRLL]} = \left[\frac{\langle |S_{HH} - S_{VV}|^2 \rangle - 4 \langle |S_{HV}|^2 \rangle}{\langle |S_{HH} - S_{VV}|^2 \rangle + 4 \langle |S_{HV}|^2 \rangle} \right] \tag{5}$$

The advantage of using only the real part of the circular coherence as compared to the complex coherence is due to the fact that the imaginary part is very sensitive to unsymmetrical scattering contributions such as vegetation (Schuler et al., 2002). Its insensitivity to dielectric constant has further been proven in several investigations (Schuler et al., 2002; Thiel, 2003).

For the spatial derivation of micro-scale soil surface roughness the Anisotropy, $|\rho_{RRLL}|$ and $Re_{[\rho RRLL]}$) were calculated by applying a 5×5 boxcar filter on the despeckled L-Band SLC data.

2.3 In-situ measurements

2.3.1 Roughness characterization

For measuring soil surface roughness a photogrammetric approach was chosen due to its efficiently with regard to a decoupled acquisition and analysis (Rieke-Zapp and Nearing, 2005). To collect samples over a wide range of roughness characteristics, soil surface roughness measurements were performed on 18 sample points (Fig. 2). Roughness characteristics ranged from smooth and crusted surfaces to ploughed and harrowed fields. For sampling roughness characteristics under vegetation, plant cover was carefully cut at the soil surface and fully removed from the field of sight of each photogrammetric image acquisition, in order to maintain an undisturbed soil surface.

For image acquisition, a Rollei d7 metric camera with known interior orientation was mounted on a tripod approximately 118 cm above the soil surface. The self-developed aluminum tripod (Fig. 3) accommodates 12 ground control points (GCP) whose three dimensional (xyz) coordinates were manually determined, as described by Lascelles et al. (2002), using a caliper rule with an accuracy of 1/10 mm. The horizontal coverage of the sampling area is limited to 70×70 cm^2 (approx. 0.5 m^2). The camera and tripod setup allows an image acquisition from 1180 mm above ground with a baseline of 480 mm resulting in a height-to-base ratio of 2.5 and an image overlap of approximately 65%, which is appropriate for roughness measurements (Rieke-Zapp and Nearing, 2005, Linder, 2006). Thus, the image block consists of two images at which the acquired images have a spatial resolution of 0.54 mm.

Digital Surface Models (DSM) were generated using Leica Photogrammetry Suite (LPS 9.0). Exterior orientation of the two images was established using high accurate GCPs and bundle block adjustment techniques. Therefore, additionally to the 12 known

GCPs, tie-points were derived and their three dimensional coordinates were calculated respectively. Best results in bundle block adjustment were achieved by using an additional 12-parameter model (Ebner, 1976). For DSM generation, LPS uses image matching strategies which work in epipolar lines (LPS, 2006). For different roughness states, adjusted matching strategies have been developed which only vary in the x direction and deliver a good fit to the known GCPs and the highly accurate tie-points. The minimum correlation coefficient for the matching process was set to 0.65, which is sufficient for epipolar line based matching algorithms (Stojic et al., 1998, Linder, 2006). In a final step, the generated DSMs were interpolated to a regular grid with a nominal resolution of 2 mm. A low-pass filter using a 7×7 kernel was applied to remove outliers.

In order to quantify soil surface roughness as a function of soil geometrical properties, roughness indices can be calculated from the derived DSM using different statistical approaches. Allmaras et al. (1966) and Currence and Lovely (1970) propose different calculation procedures based on the standard deviation of height values with additional terms to remove general slope effects. Due to the tripod geometrics, a superimposition of general slope effects can be excluded. Thus the calculation of the RMS Height can be simplified to:

$$s = \sqrt{\frac{\sum_{i=1}^{n} (Z_i - \bar{Z})^2}{1 - n}} \tag{6}$$

Where s is the RMS Height in (cm) and Z is the height values in (cm).

Some authors (Currence and Lovely, 1970; Römkens and Wang, 1986; Linden and Van Doren, 1986; Sommer, 1997) have criticized these roughness indices as these do not maintain the spatial distribution of height measurements for physical interpretation. Still, the RMS Height is the common and generally preferred index to describe soil surface roughness conditions in radar remote sensing and is thus applied in this study nonetheless (Oh et al., 1992; Hajnsek et al., 2003; Loew et al., 2006).

2.3.2 Soil and vegetation parameters

In addition to three independent intensive field campaigns over the investigation period, a broad variety of focussed in-situ measurements was carried out simultaneous to E-SAR flights. The main sampling routine included soil physical characteristics (soil moisture, roughness, bulk density) as well as vegetation parameters (wet/dry biomass, vegetation cover, plant height, LAI, shoots per m^2).

After photogrammetric image acquisition for roughness retrieval, soil samples were taken for moisture, bulk density and texture analysis. Soil moisture was measured gravimetrically using 100 cm^2 Kopecky Rings in a depth of 0–5 cm and 5–10 cm with three repetitions each. After drying at 105°C in a drying oven, volumetric soil moisture (Vol %) was calculated as well as bulk density (g*cm^{-3}) derived from the known soil volume of the Kopecky Rings.

3 Results

In Sect. 2, the methods for the retrieval of roughness information from plot scale to potential roughness estimators on the field scale were briefly described. In this section, the results from the roughness are shown and validated.

3.1 Infield roughness measurements

As described in Sect. 2.3.1, infield micro scale soil surface roughness was obtained from micro-DSMs, determined by photogrammetric image analysis. As can be seen from Fig. 5 it is possible to easily distinguish between different soil clods and even small aggregates. The bundle block adjustment revealed a sub millimeter precision for the object coordinates. Triangulation resulted in a precision of z=0.8 mm in the vertical direction and xy=0.37 mm in the horizontal direction related to the manually measured reference points. The deployed matching strategies lead to a successful matching rate

HESSD
5, 3383–3418, 2008

of approximately 72% of all possible matches in all stereo pairs. Mismatches preferably appear in areas where three main factors occur: low image contrast, soil clods obstruction in both images and strong height difference between adjacent pixels. In regions where these factors are valid, the matching algorithm fails or leads to low correlation coefficients (see Fig. 5). Indeed, the focus within the study was to develop an easy-to-apply standard procedure which allows for a rapid image acquisition near time the radar data recordings. Nevertheless, the derived DSMs showed good agreement with the high accurate reference points with a mean absolute error of 1.2 mm and a RMSE of 1.6 mm in vertical direction. Compared with literature, these accuracies are sufficiently high (Rieke-Zapp and Nearing, 2005; Wegmann et al., 2001; Warner, 1995; Taconet and Ciarletti, 2006).

Based on the micro DSM, the RMS Heights are calculated for each sample point and date using Eq. (6). Table 1 summarizes the main statistics of the calculated infield RMS Heights.

3.2 Derivation of soil surface roughness on the field scale

Figure 6 shows the comparison of the calculated potential roughness estimators, based on Eqs. (1), (5) and (6), for the 19 April 2006. The anisotropy A appears much noisier than $|\rho_{\mathrm{RRLL}}|$ and $Re_{[\rho\mathrm{RRLL}]}$. This is related to the fact that A is calculated from the second and third eigenvalues (see Eq. 1), whereas especially the third eigenvalue is a very noisy parameter (Cloude, 1999; Hajnsek, 2001; Schuler et al., 2002). The $Re_{[\rho\mathrm{RRLL}]}$ reveals the highest level of detail and does not appear as noisy as the others. Schuler et al. (2002) and Mattia et al. (1997) showed in their investigations that the polarimetric coherence decreases with an increase in surface roughness. Thus, smooth areas with sufficient backscatter intensities appear in bright colours in $|\rho_{\mathrm{RRLL}}|$ images (see Fig. 6, middle). Contrary to $|\rho_{\mathrm{RRLL}}|$, the images of $Re_{[\rho\mathrm{RRLL}]}$ show a different appearance: the values for $Re_{[\rho\mathrm{RRLL}]}$ increase with an increasing in surface roughness. Note that in contrast to A and $|\rho_{\mathrm{RRLL}}|$ values of $Re_{[\rho\mathrm{RRLL}]}$ are in the range of –1 to +1.

For the derivation of soil surface roughness on field scale, correlation coefficients

between the RMS Heights and the calculated Radar parameters have been calculated for the total investigation area; for bare soil fields and for areas with dominant surface scatter mechanisms according to Cloude and Pottier (1997). Table 2 summarizes the correlation coefficients and the coefficients of determination, showing a strong relationship only between the RMS Height and $Re_{[\rho RRLL]}$. Confirming observations obtained earlier by Thiel (2003), values with s<1 cm (ks<0.27 cm) were excluded from comparison, since these are strongly dominated by noise. On the basis of this relationship, multi temporal soil surface roughness maps have been produced.

Figure 7 shows the results of the spatial soil surface roughness derivation for the 19 April 2006. Forests, settlements and roads are masked out in light grey tones. It is possible to differentiate between rougher and smoother fields, as well as to distinguish between different in-field roughness states. However, a detailed examination of the derived soil surface roughness shows an overestimation for vegetated surfaces, especially those fields with winter rape. Figure 8 shows a scatter plot of measured versus modelled roughness values to highlight that small roughness values below ks<0.27 cm are overestimated while high in-field roughness values are underestimated by $Re_{[\rho RRLL]}$.

3.3 Multi temporal analysis of soil surface roughness

Based on this approach, multi temporal roughness maps have been calculated for each radar acquisition date. The changes in soil surface roughness over the investigation period is displayed separately for winter resistant vegetation (Fig. 9) and vegetation sown in spring (Fig. 10).

It is obvious in both figures that roughness state is changing over time. Under winter vegetation (Fig. 9), such as winter rape (101), soil surface roughness decreases slightly over the whole investigation period. For winter wheat and winter barley, a stronger decrease of roughness can be observed until the 17 May. Roughness under winter wheat stays quite low (s=1.2–1.4 cm) while the roughness state of the winter barley field increases slightly again. This backs the assumption that the roughness estimation for

the winter barley field is disturbed by vegetation. To prove this assumption, statistical analyses in form of a simple and multiple regressions showed only a minor impact (R^2=0.35) from the vegetation on the signal. As a consequence the soil surface roughness under winter resistant vegetation is overestimated by means of s=0.8 cm.

The development of roughness states for soil surface under summer vegetation (102, 460 (SB), 222 (M)) shown in Fig. 10 is similar to the winter vegetation (Fig. 9). For the maize field (222) a slight decrease can be observed, which is similar to the trend of the in-field photogrammetric roughness measurements. Indeed, the infield roughness values for s are 0.2 cm higher than the estimated roughness values.

Both of the sugar beet fields (102, 460) show a strong increase in roughness from the first campaign date to the second, which is related to agricultural practice, respectively seed bed preparation. Afterwards, a decrease in soil surface roughness until the 17 May can be observed, before showing a continuous increase very similar to the growth of the sugar beet plants. However, a multiple regression between the roughness values, standard vegetation parameters and $Re_{[p\mathrm{RRLL}]}$ showed only a strong relationship between the values on field 460 (R^2=0.68). On field 102 there was no significant relationship (R^2=0.11). For the sugar beet fields, an average overestimation of roughness can be observed of 0.21 cm for field 102 and 0.26 cm for 460.

4 Potentials for hydrological model application

This section discusses the potentials and limitations of the proposed roughness retrieval for direct use in hydrological models. Results of a feasibility study of using roughness information in physically based hydro-ecological modeling will be presented. First, micro depressional storage capacity is calculated using a set of simple equations proposed by Onstad (1984) and Kamphorst (2000). In addition, the retrieval of soil porosity as well as of the void ratio using soil surface roughness information is investigated.

4.1 Estimation of water retention and detention using roughness data

Storage capacity in micro depressions is a crucial parameter in physically-based flood forecasting models (Hansen et al., 1999; Kamphorst et al., 2000; Planchon et al., 2001) since it plays an important role in overland flow generation and runoff velocity. However, until now, there is no adequate direct measuring method available (Onstadt, 1984; Linden et al., 1998; Kamphorst et al., 2000; Rieke-Zapp and Nearing, 2005). Onstadt (1984) and Kamphorst et al. (2000) developed simple inversion approaches using the RMS Height for the calculation of the micro depressional storage capacity.

Maximum storage capacity is calculated by Onstad (1984) using the following equation:

$$\mathrm{MDS}_{\mathrm{Onstad}} = 0.112 \times s + 0.031 \times s^2 - 0.12 \times s \times \mathrm{slope}(\%) \quad (7)$$

Where MDS is the maximum depressional storage capacity in (cm), s is the RMS Height (cm) of a given area (e.g. Pixel) and slope(%) is the slope in percent calculated from a digital terrain model. In addition to Onstad (1984), Kamphorst et al. (2000) calculated the maximum storage capacity using a linear fit (R^2=0.8):

$$\mathrm{MDS}_{\mathrm{Kamphorst}} = s \times 0.28 \quad (8)$$

The amount of precipitation required to fill all depressions within a resolution cell MDSexcess is calculated as (Onstadt, 1984):

$$\mathrm{MDSexcess} = 0.329 \times s + 0.073 \times s^2 - 0.018 \times s \times \mathrm{slope}(\%) \quad (9)$$

In the absence of infiltration (infiltration=0), the rainfall excess needed to start surface runoff STARTRUN (cm) is determined using the following equation defined by Cremers et al. (1996)

$$\mathrm{STARTRUN} = \mathrm{MDSexcess} \times [0.0527 \times s - 0.0049 \times \mathrm{slope}(\%)] \quad (10)$$

Figure 11 shows examples for the spatial distribution of MDS and STARTRUN, based on Eqs. (8) and (10), using the spatially derived soil surface roughness information

HESSD
5, 3383–3418, 2008

described in Sect. 3. It can be seen in detail that the slope gradient is the main driving variable for depression storage calculations. As a result of the different roughness conditions within the fields, e.g. field 460, different values can be determined, depending on the well derived spatial distribution of roughness information: While the northern parts of field 460 are still crusted, thus showing lower MDS values, the southern parts are already tilled and thus much rougher, leading to higher MDS values. Consequently, this source of information for overland flow assessment can contribute to an improved accuracy of flood modeling systems which are capable to interpret high-resolution, spatially distributed model parameters.

4.2 Estimation of soil bulk density, porosity and void ratio using roughness information

In addition to soil texture (grain size), bulk density and derived variables such as porosity and void ratio are key parameters in hydrological modelling. Most widely used pedotransfer- functions (PTF) for the calculation of hydro-ecological properties such as (un-) saturated conductivity are based on these parameters (Cosby et al., 1984; Rawls and Brakensiek, 1985; Woesten et al., 1999; Sobieraj et al., 2001). Further, porosity as well as void ratio are important indicators for the detection of mechanically compacted soils in agricultural environments. Typically, bulk density can be determined using Kopecky rings with known volume, while soil porosity is mainly measured using an air pycnometer (Schlichting et al., 1998; Sun et al., 2006). Alternatively, soil porosity (n) as well as void ratio (ε) can be calculated from bulk density measurements using the following equations (Hartge and Horn, 1999):

$$n = 1 - \frac{\rho_s}{\rho_F} \tag{11}$$

$$\varepsilon = \frac{n}{1 - n} \tag{12}$$

Where n denotes soil porosity in (%); ρ_s is the bulk density of the given soil (g*cm^{-3}) and ρ_F is the bulk density of the solid particles, where for quartzous soils

$\rho_F \approx 2.65\,\mathrm{g^*cm^{-3}}$.

However, there are some drawbacks in using these classical methods. First, using destructive measurements such as Kopecky rings or the air pycnometer do not allow a multi temporal analysis. Secondly, they are limited to a small area (plot scale) and therefore time-, labor- and cost-consuming for field scale assessments.

Sun et al. (2006) introduced the potential of using roughness information for the derivation of soil porosity. Using a linear fit, they predicted porosity from RMS Heights for different roughness conditions of a silty loam. The hypothesis is based on the assumption that changing roughness due to tillage or precipitation alters only volume but not mass of the soil column (Hartge and Horn, 1999) and thus introduces a change in soil porosity.

To verify the approach suggested by Sun et al. (2006), the correlation between the in-field roughness measurements and the bulk parameters calculated from Eqs. (11) and (12) are determined. To avoid any influence from vegetation, only bare fields were considered. Table 3 summarizes the statistics from this analysis.

A good relationship between the indicated parameters can be noted, while the void ratio in the uppermost layer is correlated stronger to s than the bulk density and porosity. This is in good agreement with the results of Sun et al. (2006). While the spatial derivation of these parameters on field 460 for the 19 April leads to plausible estimates (Fig. 12) using the proposed approach, this procedure is only a first quality assessment and requires further research.

5 Summary and conclusions

This study presents an approach for the spatial derivation of soil surface roughness using photogrammetry and radar remote sensing. It is shown that the deployed method allows a fast and adequate retrieval of roughness information on bare soils. In presence of vegetation cover, the retrieval algorithm leads to an overestimation of roughness and is therefore not suitable for operational use. Even though an influence on $Re_{[RRLL]}$ from

vegetation could not be quantified with the available standard vegetation parameters, it is obvious that plant growth affects the estimation of s by means of $Re_{[RRLL]}$. Hence, the algorithm works fairly well on bare soils, which confirms the investigation of Schuler et al. (2002) and Thiel (2003). Indeed, the overestimation of roughness under vegetation, as explained above, is contrary to the investigations of Schuler et al. (2002) and Thiel (2003)

Considering these limitations, the derived roughness information is used to calculate micro depression storage capacity (MDS) as a potential parameter for hydro-ecological modelling. Results indicate that an incorporation of spatially determined soil surface roughness from remote sensing can support the parameterization of spatially explicit hydrologic models, in this case by providing distributed values of driving variables.

In addition, it is shown in a first assessment that soil bulk parameters of the upper few centimetres of the soil column, such as bulk density, porosity and void ratio, can be discriminated from surface roughness. However, even though a dependency of these bulk parameters from roughness can be noted, the approach needs further research with regard to different uncertainties:

- The correlation between roughness parameters and bulk parameters is only strong for fresh harrowed fields. For small values of $s \leq 1$ cm the bulk parameters are randomly distributed.
- Using the regionalization approach suggested in this study, error propagation will lead to large RMSE values. Therefore, a better roughness retrieval has to be achieved.

Nevertheless, the approach is very promising for bare soil fields. For future investigations, an enhanced roughness retrieval has to comprise two major improvements:

- To enhance the in-field roughness retrieval, the image acquisition set up has to be improved by better illumination and to solve the appearance of obstructed areas more than two image pairs could remediate (Luhmann, 2003; Wiggenhagen and

Raguse, 2003). To face the problem of mismatches between adjacent pixels with strong height differences, a broad variety of appropriate matching strategies have to be developed to enhance the matching process.

– For a better separation of vegetation effects different decomposition theorems as well as deploying PolInSAR techniques will be necessary.

Acknowledgements. The authors would like to thank ESA for funding the AgriSAR 2006 campaign. D. Rieke-Zapp (University of Bern) is gratefully acknowledged for providing the Rollei d7 metric camera and for assistance and support during the photogrammetric processing.

References

Allmaras, R. R., Burwell, R. E., Larson, W. E., and Holt, R. F.: Total porosity and random roughness of the interrow zone as influenced by tillage, USDA Conservation Research Report, 7, 1966.

Bertuzzi, P., Rauws, G., and Courault, D.: Testing roughness indices to estimate soil surface roughness changes due to simulated rainfall, Soil Till Res., 17, 87–99, 1990.

Cerdan, O., Souchère, V., Lecomtze, V., Couturier, A., and Le Bissonnais, Y.: Incorporating soil surface crusting processes in an expert-based runoff model: Sealing and Transfer by Runoff and Erosion related to Agricultural Management – STREAM. Catena Vol., 189–205, 2001.

Cloude, S. R.: Eigenvalue parameters for surface roughness studies. Proceedings of SPIE Conference on Polarization: Measurement, analysis and remote Sensing II. Denver, Colorado, 1999.

Cloude, S. R. and Lewis, G. D.: Eigenvalue Analysis of Mueller Matrix for Bead Basted Aluminium Surfaces, SPIE Polarisation Analysis and Measurement III, Proceedings of SPIE, AM107, July–August, 2000.

Cloude, S. R. and E. Pottier: A review of target decomposition theorems in radar polarimetry, IEEE Trans. Geosci. Remote Sens., 34, 498–518, 1996.

Cloude, S. R. and Pottier, E.: An entropy based classification scheme for land applications of polarimetric SAR, IEEE Trans. Geosci. Remote Sens., 35(1), 68–78, 1997.

Cosby, B. J., Hornberger, G. M., Clapp, R. B., and Ginn, T. R.: A statistical exploration of the

relationships of soil moisture characteristics to the physical properties of soils, Water Res. Res., 20, 682–690, 1984.
Cremers, N. H. D. T., Van Dijk, P. M., De Roo, A. P. J., and Verzandvoort, M. A.: Spatial and temporal variability of soil surface roughness and the application in hydrological and soil erosion modelling, Hydr. Proc., 10, 1035–1047, 1996.
Currence, H. D. and Lovely, W. G.: The analysis of soil surface roughness, Trans. ASAE, 13, 710–714, 1970.
Darboux, F., Gascuel-Odoux, C. and Davy, P.: Effects of surface water storage by soil roughness on overland-flow generation, Earth Surf. Proc. Landforms, 27, 223–233, 2002.
Ebner, H.: Self calibrating block adjustment. Proceedings XIII Congress of the International Society of Photogrammetry, Helsinki, 1976.
Farres, P. J.: Some observations on the stability of soil aggregates to raindrop impact, Catena 7, 223–231, 1980.
Fohrer, N., Berkenhagen, J., Hecker, J.-M., and Rudolph, A.: Changing soil and surface conditions during rainfall single rainstorms/subsequent rainstorms, Catena, 37, 355–375, 1999.
Hajnsek, I., Bianchi, R., Davidson, M., Durso, G., Gomez-Sanchez, J., Hausold, A., Horn, R., Howse, J., Loew, A., Lopez-Sanchez, J., Ludwig, R., Martinez-Lozano, J., Mattia, F., Miguel, E., Moreno, J., Pauwels, V., Ruhtz, T., Schmullius, C., Skriver, H., Sobrino, J., Timmermans, W., Wloczyk, C., and Wooding, M.: AgriSAR 2006 Airborne SAR and Optics Campaigns for an improved monitoring of agricultural processes and practices, European Geoscience Union (EGU), General Assembly, 15–20 April 2007, Vienna, Austria, 2007.
Hajnsek, I., Pottier, E., and Cloude, S. R.: Inversion of surface parameters from polarimetric SAR, IEEE Trans. Geosci. Remote Sens., 41, 727–744, 2003.
Hansen, B., Schjønning, P., and Sibbesen, E.: Roughness indices for estimation of depression storage capacity of tilled soil surfaces, Soil Till. Res., 52, 103–111, 1999.
Hartge, K. H. and Horn, R.: Einführung in die Bodenphysik, 3. Auflage, Ferdinand Enke, Stuttgart, 1999.
Helming, K.: Die Bedeutung des Mikroreliefs für die Regentropfenerosion, Bodenökologie und Bodengenese Nr. 7, Berlin, 1992.
Kamphorst, E. C., Jetten, V., Gue'rif, J., Pitkänen, J., Iversen, B. V., Douglas, J. T., and Paz, A.: Predicting depressional storage capacity from soil surface roughness, Soil Sci. Soc. Am. J., 64, 1749–1758, 2000.
Lascelles, B., Favis-Mortlock, D., Parsons, T., and Boardman, J.: Automated digital pho-

togrammetry: a valuable tool for small-scale geomorphological research for the non-photogrammetrist?, Trans. GIS, 6, 5–15, 2002.
Le Bissonnais, Y., Benkhada, Chaplot, V., Fox, D., King, D., and Daroussin, J.: Crusting, runoff and sheet erosion on silty loamy soils at various scales and upscaling from m^2 to small catchments, Soil Till. Res., 46, 69–80, 1998.
Linden, D. R. and Van Doeren, D. M.: Parameters for characterizing tillage induced soil surface roughness, Soil Sci. Soc. Am. J., 50, 1560–1565, 1986.
Linder, W.: Digital Photogrammetry, A Practical Course, Springer Berlin, Heidelberg, New York, 2006.
LPS: Leica Photogrammetry Suite User Manual V 9.0, 2006.
Loew, A., Ludwig, R., and Mauser, W.: Derivation of surface soil moisture from ENVISAT ASAR WideSwath and Image mode data in agricultural areas. IEEE Trans. Geosci. Remote Sens., 44, 889–899, 2006.
Loew, A. and Mauser, W.: Inverse modeling of soil characteristics from surface soil moisture observations: potential and limitations, Hydrol. Earth Syst. Sci. Discuss., 5, 95–145, 2008, http://www.hydrol-earth-syst-sci-discuss.net/5/95/2008/.
Luhmann, T.: Nahbereichsphotogrammetrie – Grundlagen, Methoden und Anwendungen. Heidelberg, 2003.
Mattia, F., Le Toan, T., Souyris, J.C., De Carolis, G., Floury, N., Posa F., and Pasquariello, G.: The effect of surface roughness on multi- frequency polarimetric SAR data. IEEE Trans. Geosci. Remote Sens., 35, 954–966, 1997.
Oh, Y., Sarabandi, K., and Ulaby, F. T.: An empirical model and an inversion technique for rader scattering from bare soil surfaces, IEEE Trans. Geosci. Remote Sens., 30, 370–381, 1992.
Onstad, C. A.: Depressional storage on tilled surface, Trans. ASAE, 27, 729–732, 1984
Planchon, O., Esteves, M., Silvera, N., and Lapetite, J. M.: Microrelief induced by tillage: measurement and modelling of surface storage capacity, Catena, 46, 141–157, 2001.
Rawls, W. and Brakensiek, D.: Prediction of soil water retention properties for hydrologic modelling, Watershed Management in the Eighties, Proc. Symposium of Irrig. Drainage Div. ASCE, Denver, CO., 30 April–1 May 1985, 293–299, 1985.
Rieke-Zapp, D. and Nearing, M. A.: Digital close range photogrammetry for measurement of soil erosion, The Photogrammetric Record, 20, 69–87, 2005
Römkens, M. J. and Wang, J. Y.: Effect of tillage on surface roughness, Trans. ASAE 29, 429–433, 1986.

Santanello, J. A., Peters-Lidard, C. D., Garcia, M. E., Mocko, D. M., Tischler, M. A., Moran, S., and Thoma, D.: Using remotely-sensed estimates of soil moisture to infer soil texture and hydraulic properties across a semi-arid watershed, Rem. Sens. Env., 110, 79–97, 2007.

Scheiber, R., Keller, M., Fischer, J., Horn, R., and Hajnsek, I.: Radar Data Processing, Quality Analysis and Level-1b Product Generation for AGRISAR and EAGLE campaigns. Proceedings AGRISAR and EAGLE Campaigns Final Workshop, 15–16 October 2007, ESA/ESTEC , Noordwijk, the Netherlands, CD, 2007.

Schlichting, E., Blume, H. P., and Stahr, K.: Bodenkundliches Praktikum, Blackwell, Berlin, 1995.

Schuler, D. L., Lee, J. S., and Kasilingam, D.: Surface roughness and slope measurements using polarimetric SAR data, IEEE Trans. Geosci. Remote Sens., 40, 687–698, 2002.

Sobieraj, J. A., Elsenbeer, H., and Vertessy, R. A.: Pedotransfer functions for estimating saturated hydraulic conductivity: implications for modelling storm flow generation, J. Hydrol., 251, 202–220, 2001.

Sommer, H.: Quantifizierung der Rauigkeit von Bodenoberflächen und Simulation hydromechanischer Prozesse anhand von Oberflächenmodellen, Aachen, 1997.

Sun, Y., Lin, J., Schulze Lammers, P., and Damerow, L.: Short communication, Estimating surface porosity by roughness measurement in a silt – loam field, J. Plant Nutr. Soil Sci., 169, 630–632, 2006.

Taconet, O. and Ciarletti, V.: Estimating soil roughness indices on a ridge-and-furrow surface using stereo photogrammetry, Soil Till. Res., 93, 64–76, 2006.

Thiel, C.: Measuring surface roughness on base of the circular polarization coherence as an input for simple inversion of the IEM model. Proceedings of PolInSAR Workshop, 14–16 Januray 2003, Frascati, Italy 2003.

Thiel, C., Gruenler, S., Herold, M., Hochschild, V., Jaeger, G., and Hellmann, M.: Interpretation and Analysis of Polarimetric L-Band E-SAR-Data for the Derivation of Hydrologic Land Surface Parameters, IEEE Proceedings IGARSS'01, Sydney, CD, 2001.

Warner, W. S.: Mapping a three-dimensional soil surface with handheld 35 mm photography. Soil Till. Res., 34, 187–197, 1995.

Wegmann, H., Rieke-Zapp, D., and Santel, F.: Digitale Nahbereichs-photogrammetrie zur Erstellung von Oberflächenmodellen für Bodenerosionsversuche. Publikationen der Deutschen Gesellschaft für Photogrammetrie und Fernerkundung, 9, 2001.

Wiggenhagen,. M. and Raguse, K.: Entwicklung von Kenngrößen zur Qualitätsbeurteilung op-

tischer Prozessketten, PFG, 2, 125–134, 2003.
Woesten, J.: Soil Quality for Crop Production and Ecosystem Health, Development in Soil Science, chap. Pedotransfer functions to evaluate soil quality, 221–245, Elsevier, 1997.
Zeiger, M.: Assessment of dynamic biotic and abiotic processes at the soil surface affected by different management systems, Kiel, 2007.

Table 1. Statistical characteristics for RMS Heights.

Parameter	*s*
STD	0.45
Mean	1.27
Mod	0.9
Med	1.0
Max	3.3
Min	0.6

Table 2. Correlation between s and calculated PolSAR parameters.

Parameter	s	
	r	R^2
$\text{Anisotropie}_{\text{surface scatt.}}$	0.05	0.00
$\text{Anisotropie}_{\text{bare soil}}$	0.09	0.00
$\lvert\rho\text{RRLL}\rvert_{\text{total}}$	–0.419	0.176
$\lvert\rho\text{RRLL}\rvert_{\text{surface scatter}}$	–0.257	0.066
$\lvert\rho\text{RRLL}\rvert_{\text{bare soil}}$	–0.361	0.13
$Re_{[\rho\text{RRLL}]\text{total}}$	0.709	0.502
$Re_{[\rho\text{RRLL}]\text{surface scatter}}$	0.525	0.276
$Re_{[\rho\text{RRLL}]\text{bare soil}}$	0.726	0.528

Table 3. Correlation between s and soil bulk density parameters (R^2=coefficient of determination, r=correlation coefficient, m=slope, b=axis intercept).

Parameter	R^2	r	m	b
ρ_s	0.55	–0.74	–0.32	1.90
n	0.55	0.74	12.14	28.28
ε	0.60	0.78	0.49	0.16

HESSD
5, 3383–3418, 2008

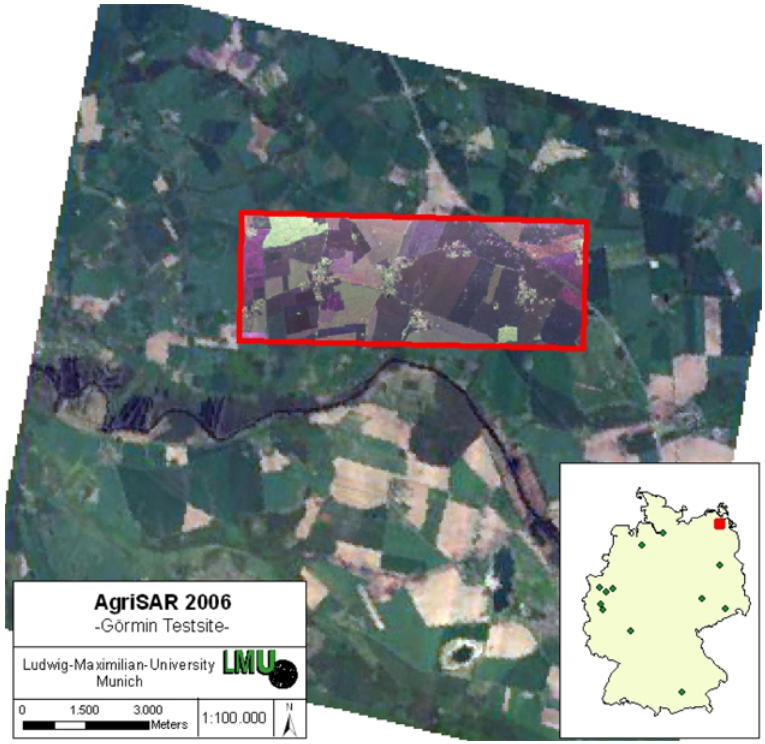

Fig. 1. Overview of DEMMIN-Görmin Testsite in the North East of Germany.

HESSD
5, 3383–3418, 2008

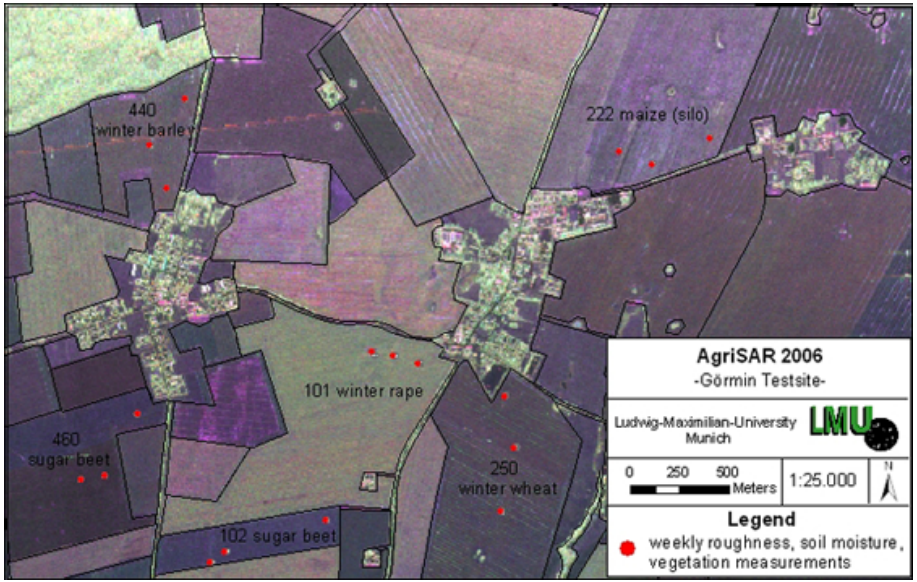

Fig. 2. Location of sample points within the Görmin Testsite during AgriSAR 2006.

HESSD
5, 3383–3418, 2008

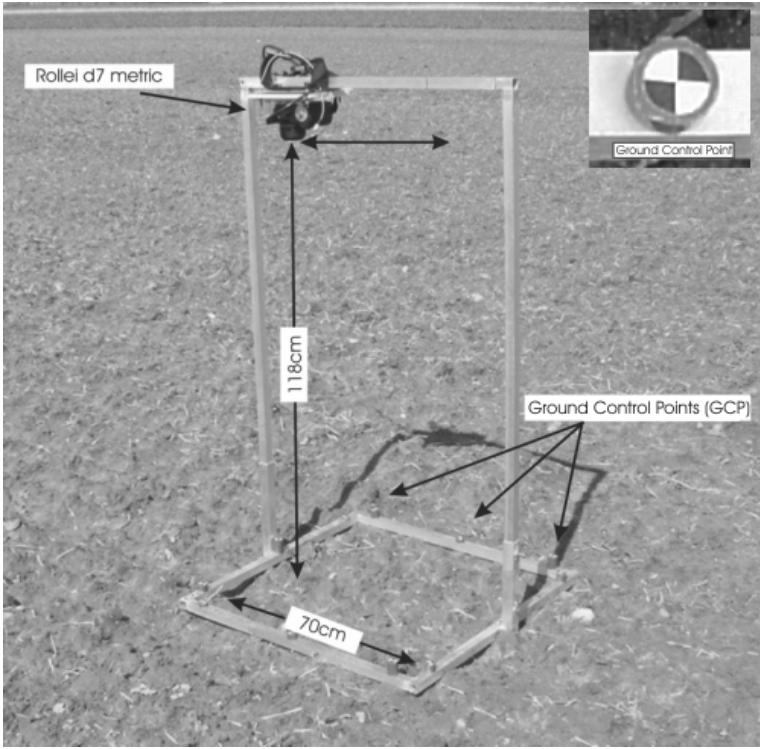

Fig. 3. Camera system for photogrammetric image acquisition (setup and signalized control point).

HESSD
5, 3383–3418, 2008

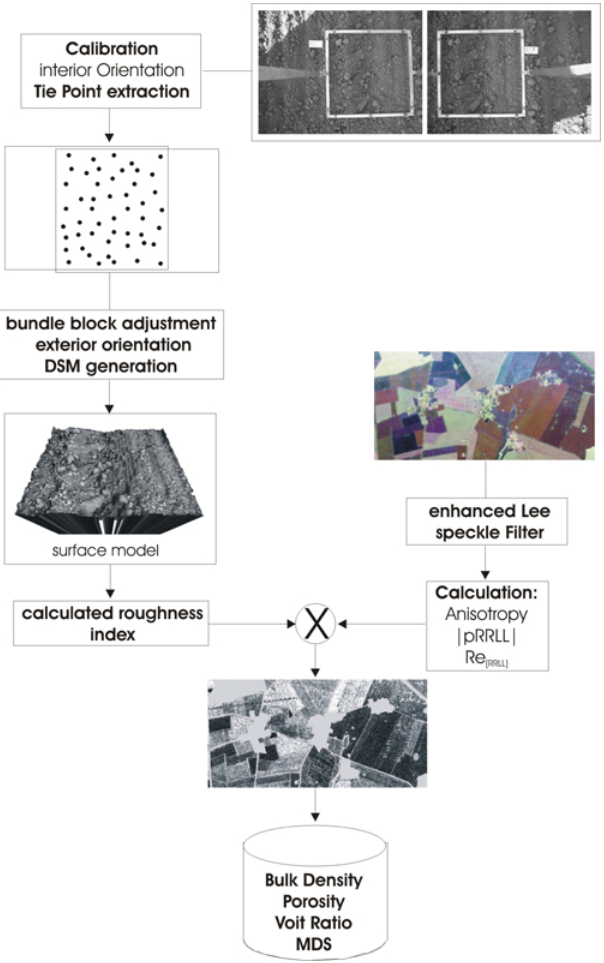

Fig. 4. Scheme for roughness retrieval approach.

HESSD
5, 3383–3418, 2008

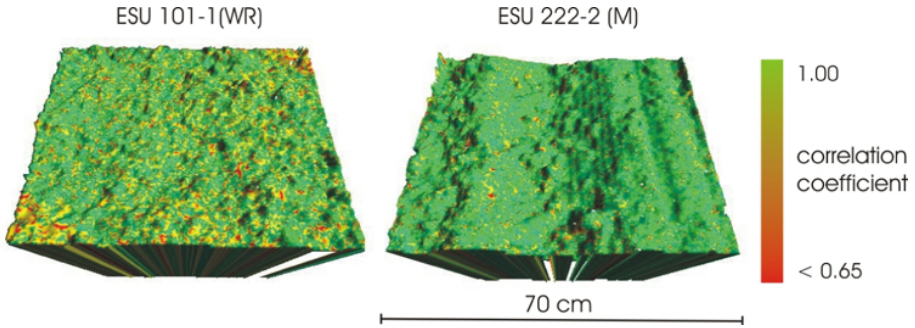

Fig. 5. Correlation coefficients of the matching process for two different sample points (101-1/222-2) and roughness states.

HESSD
5, 3383–3418, 2008

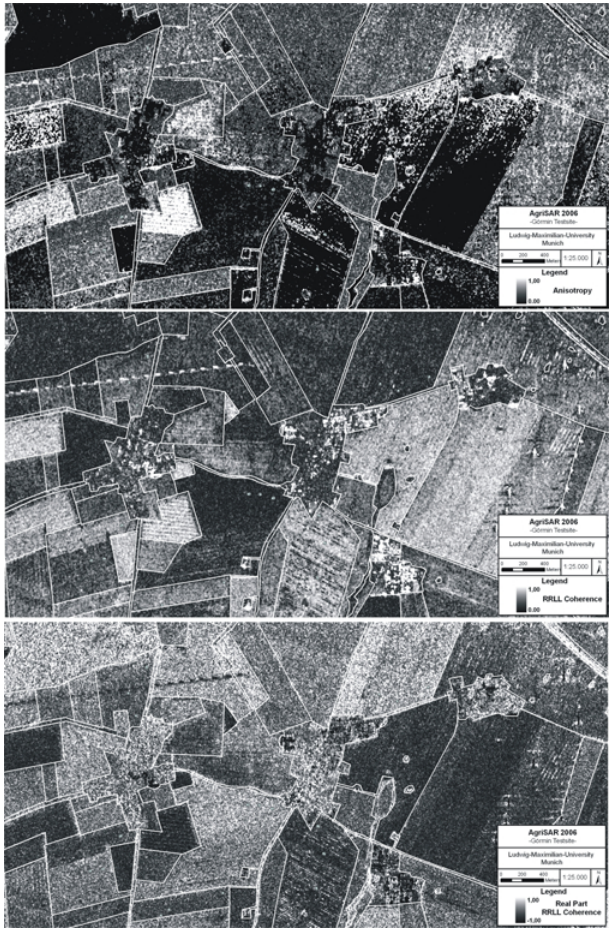

Fig. 6. Calculated roughness estimators (Anisotropy, Circular Coherence and Real Part of the Circular Coherence) for the 19 April 2006.

HESSD

5, 3383–3418, 2008

Surface roughness derivation from PolSAR data

P. Marzahn and R. Ludwig

Fig. 7. Derived RMS Heights from the relation between the $Re_{[\rho RRLL]}$ and the in-field soil surface roughness.

HESSD
5, 3383–3418, 2008

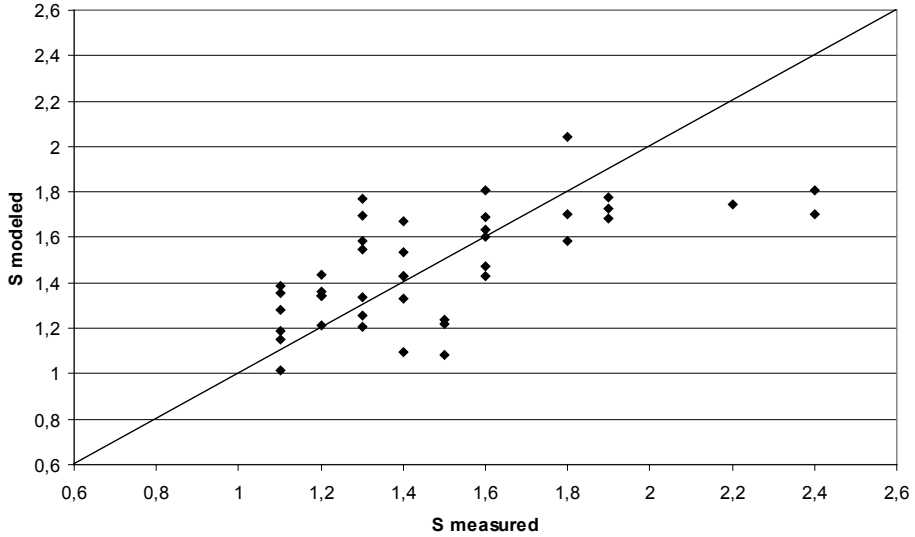

Fig. 8. Modeled versus measured soil surface roughness values.

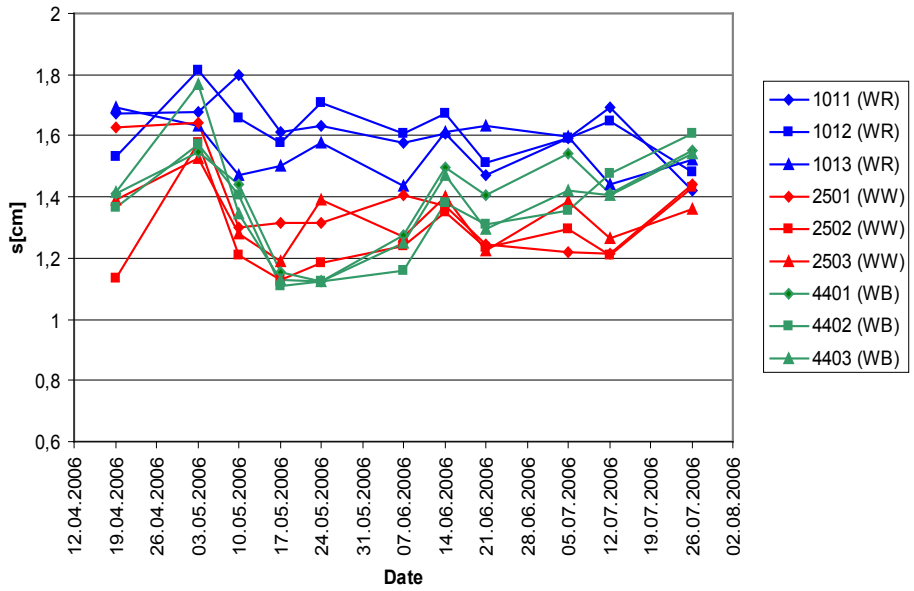

Fig. 9. Temporal development of derived RMS Heights for winter resistant vegetation (winter wheat, barely, rape).

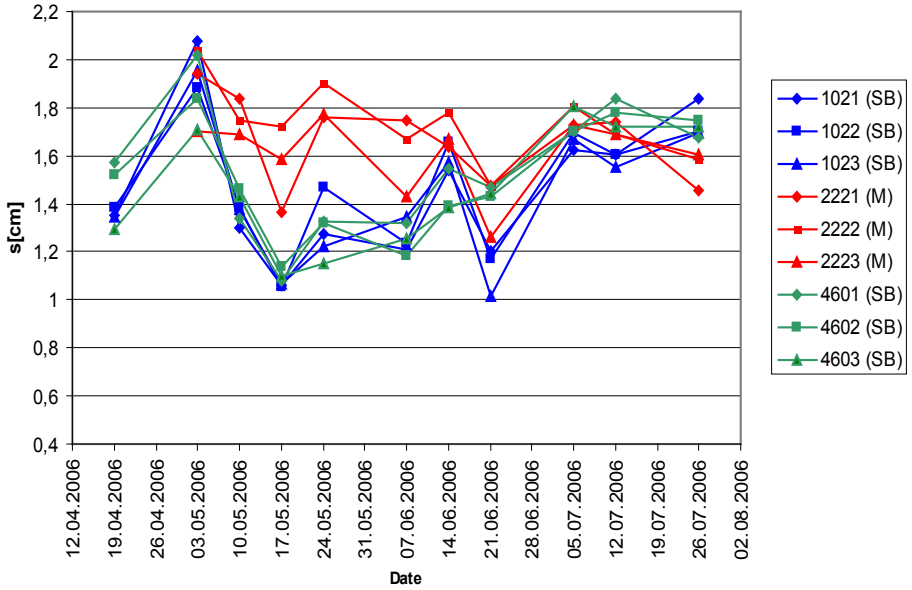

Fig. 10. Temporal development of derived RMS Heights under summer vegetation (maize, sugar beet).

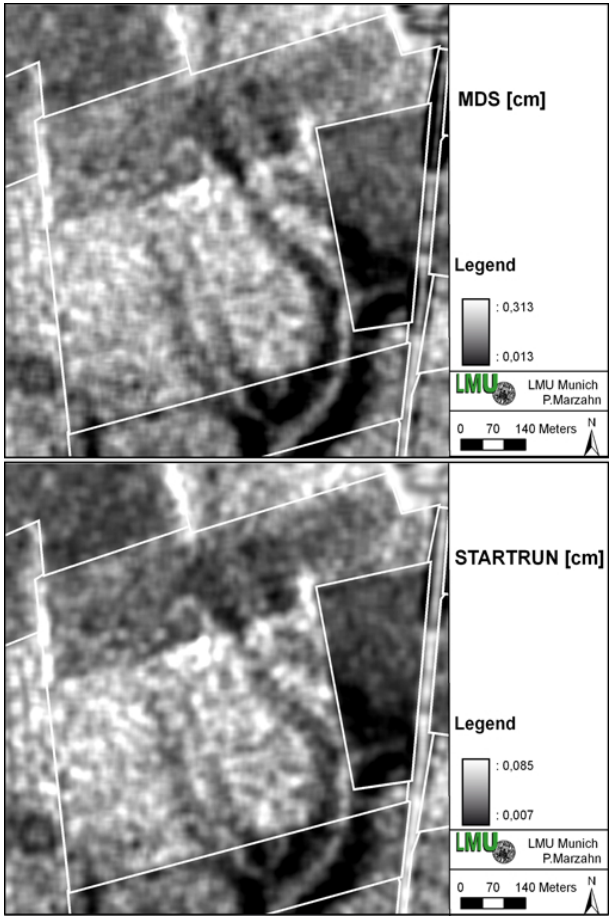

Fig. 11. Calculated maximum depression storage (MDS) and point to start runoff (STARTRUN) for Field 460 at the 19 April 2006.

HESSD
5, 3383–3418, 2008

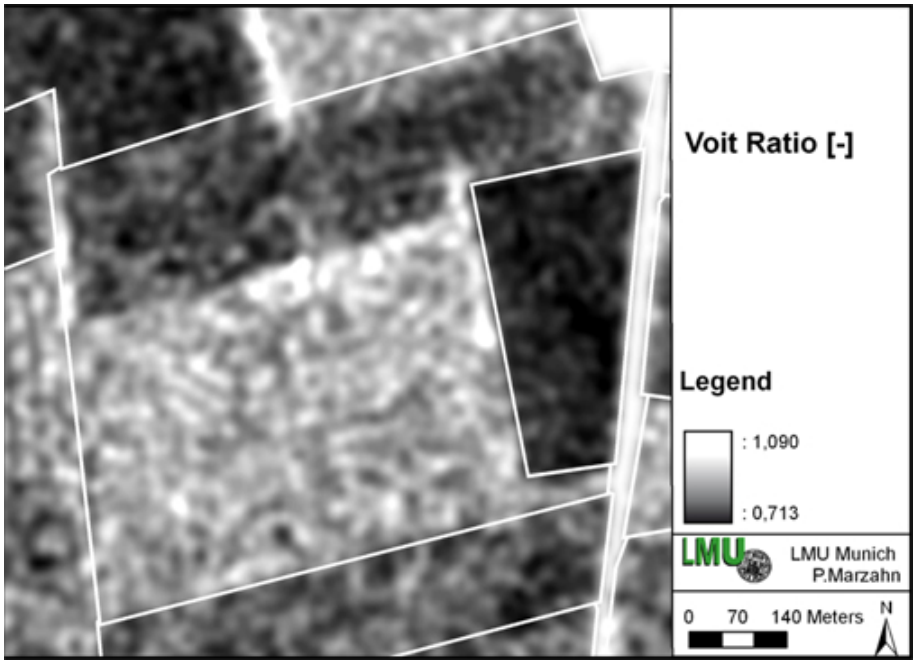

Fig. 12. Results for the regionalization of bulk parameters on Field 460 using soil surface roughness information.

HESSD
5, 3383–3418, 2008